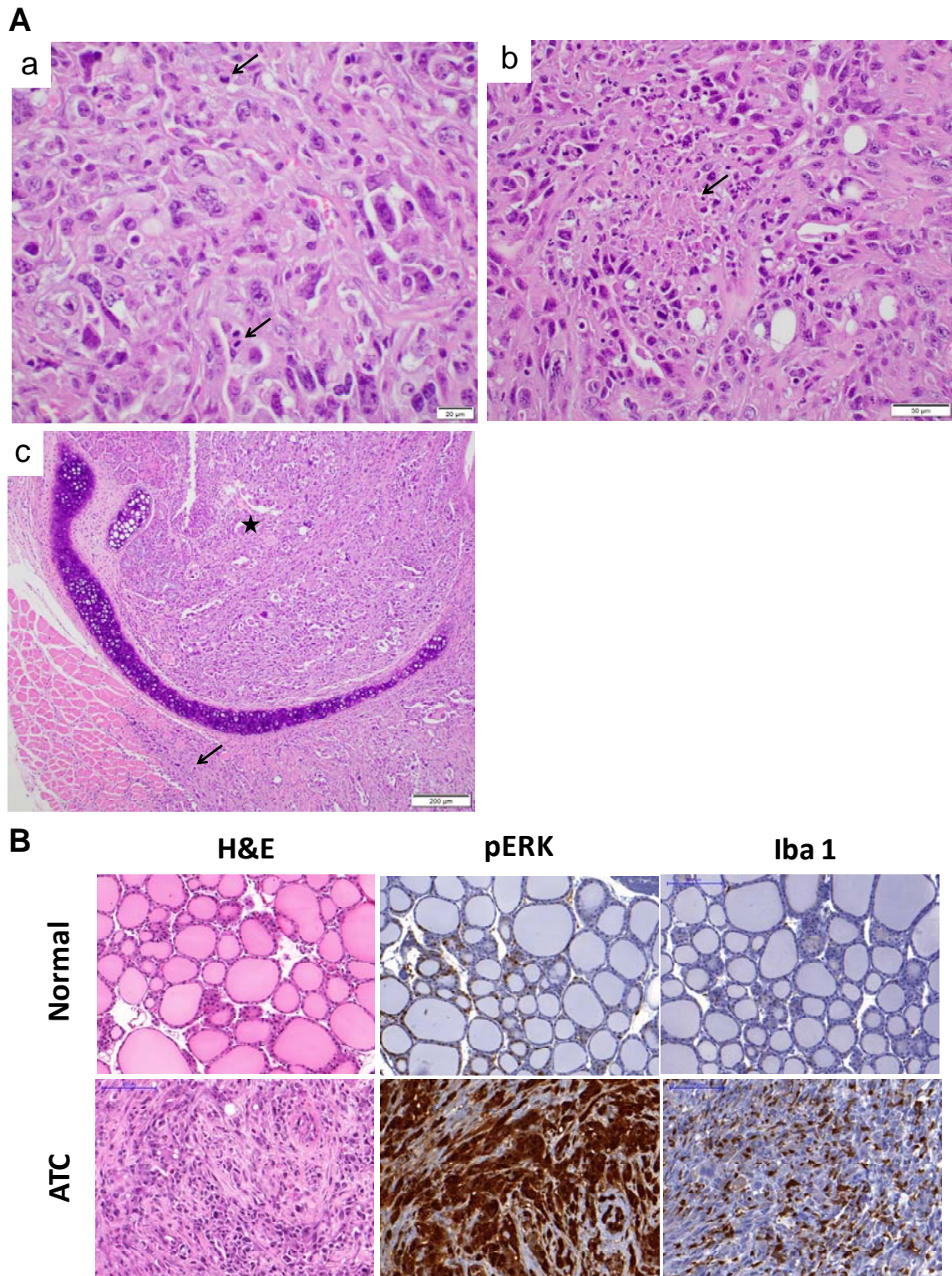


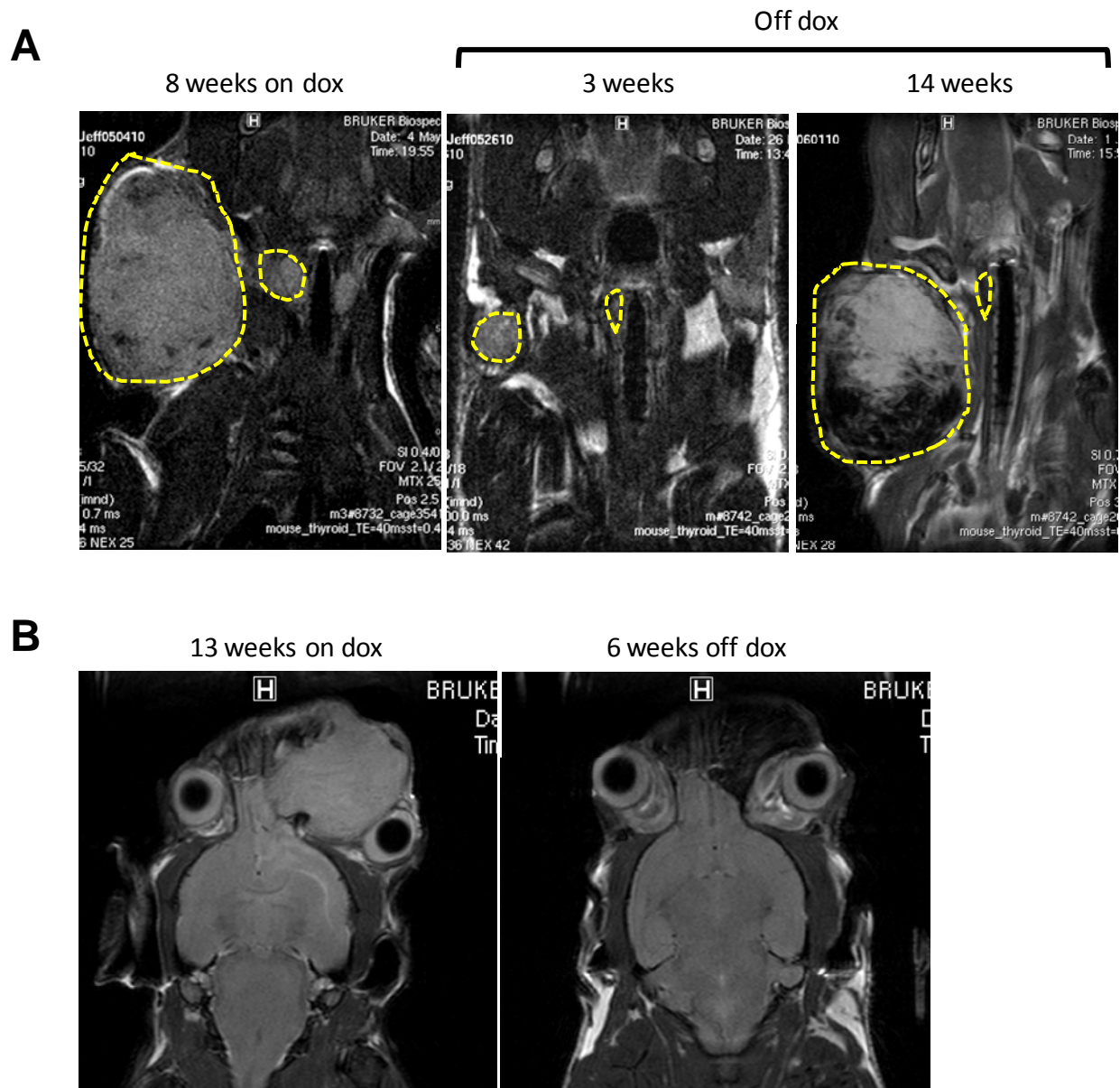
Supplemental Figure 1: MAPK transcriptional output is increased in the transition from PTC to ATC. A) Quantitative RT-PCR with primers that amplify both mouse and transgenic human BRAF using RNA isolated from the thyroid tissue of the *TPO-Cre/LSL-rtTA* and dox-treated (1 week) *TPO-Cre/LSL-rtTA/teto-Braf^{V600E}* mice. **B)** MAPK transcriptional output of tumors from the following mouse models: Knauf, *TPO-Cre/LSL-Braf^{V600E}* (PTC, *Braf^{V600E}* knock-in model (1) and *BRAF/p53* (ATC); McFadden (GSE55933, *Braf^{V600E}* knock-in model), tamoxifen-treated *TPO-Cre^{ER}/Braf^{CA/+}* (PTC) and *TPO-Cre^{ER}/Braf^{CA/+}/Trp53 Δ ex2-10/ Δ ex2-10* (ATC) (2); Human *BRAF^{V600E}* mutant PTCs and ATCs (GSE33630 and GSE76039). **C,D)** Quantitative RT-PCR with primers that amplify both mouse and transgenic BRAF (C) or rTA (D) using RNA isolated from thyroid tissue of normal mice and dox-treated (8 weeks) *BRAF/p53* mice with or without ATC. Tumor-free mice commonly exhibited hyperplasia (hyp). **E)** Braf expression in tamoxifen-treated *TPO-Cre^{ER}/Braf^{CA/+}* (PTCs) and *TPO-Cre^{ER}/Braf^{CA/+}/Trp53 Δ ex2-10/ Δ ex2-10* (ATCs) (GSE55933) (2).

References

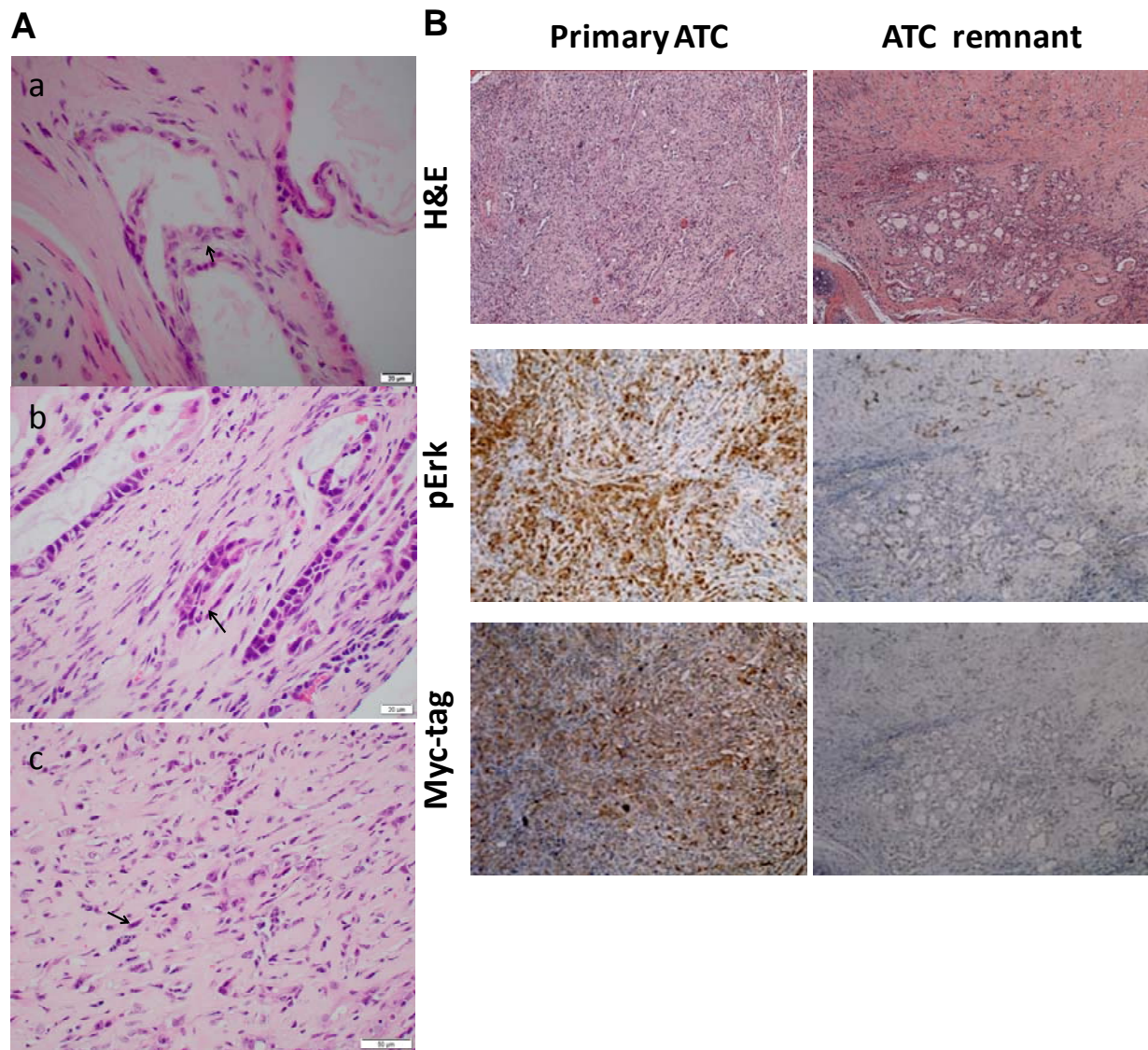
1. Franco, A. T. *et al.* (2011) Thyrotrophin receptor signaling dependence of Braf-induced thyroid tumor initiation in mice *Proc. Natl. Acad. Sci. U. S. A.* **108**, 1615-1620.
2. McFadden, D. G. *et al.* (2014) p53 constrains progression to anaplastic thyroid carcinoma in a Braf-mutant mouse model of papillary thyroid cancer *Proc. Natl. Acad. Sci. U. S. A.* **111**, E1600-E1609.



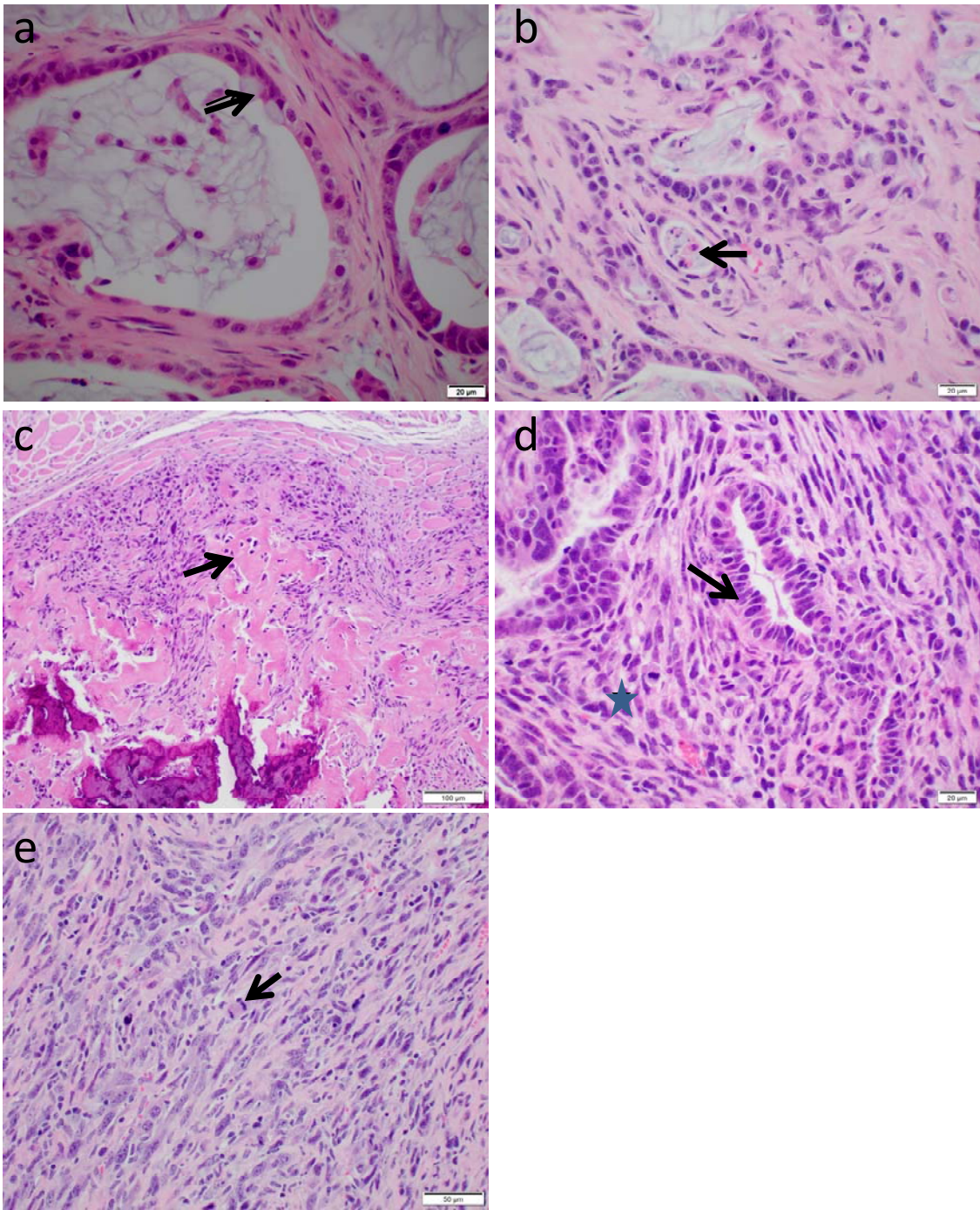
Supplemental Figure 2: ATC features of *BRAF/p53* mice. **A)** H&E staining of thyroid sections from *BRAF/p53* mice on dox for 7-10 weeks showing (arrows): a) mitosis; b) necrosis and c) muscle invasion. Star in panel c shows tracheal invasion. **B)** IHC for pERK and the macrophage marker Iba1 in normal thyroid and an ATC from a *BRAF/p53* mouse.



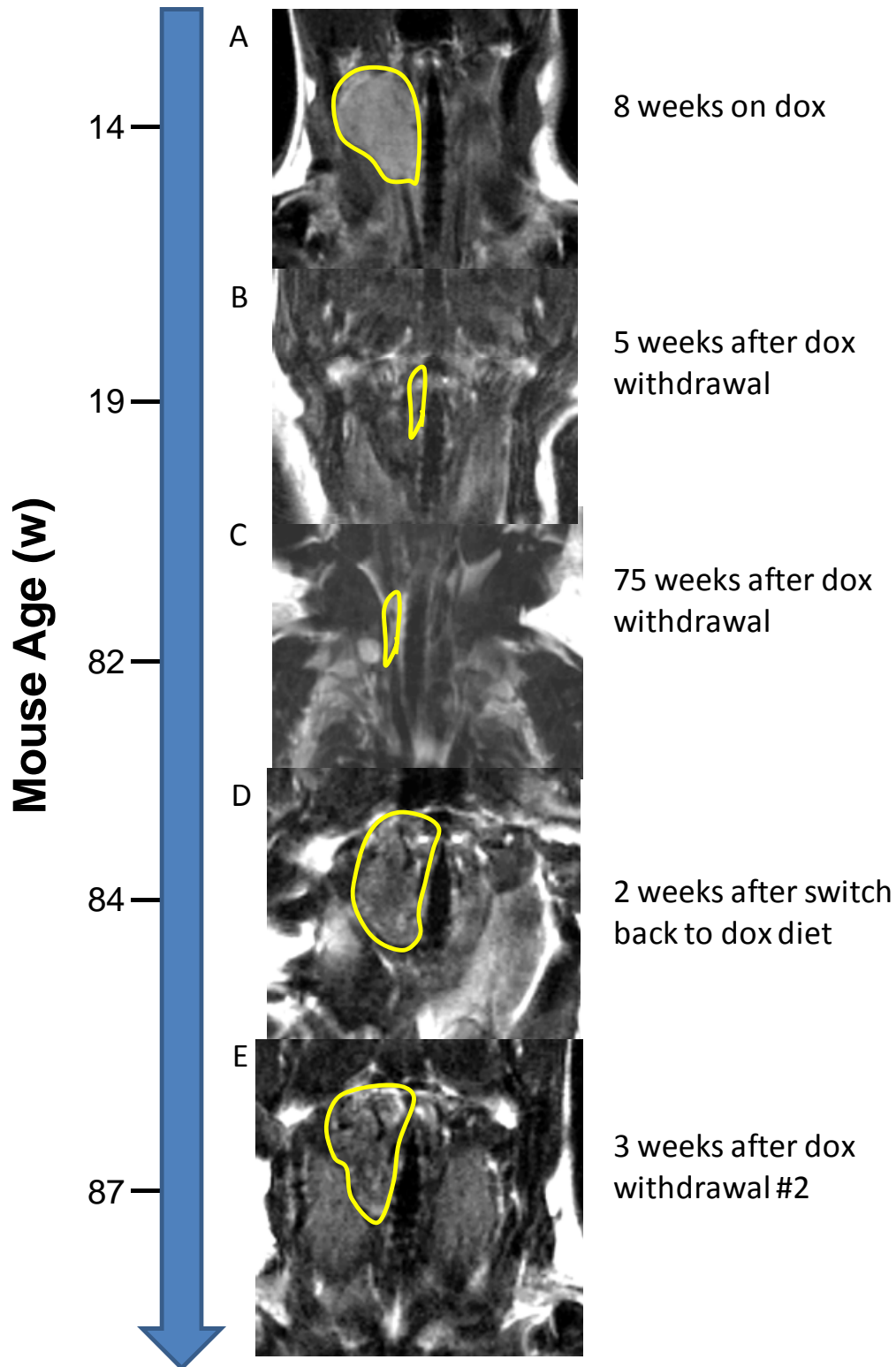
Supplemental Figure 3: Metastases from ATCs of *BRAF/p53* mice are addicted to the oncoprotein. A) MRI images of a primary ATC and a lymph node metastasis detected 8 weeks after switching to dox-impregnated chow (*left*). MRI showing regression of primary tumor and the lymph node metastasis 3 weeks after switching to dox-free diet (*middle*). Recurrence of lymph node in MRI performed 11 weeks later (*right*). **B) Left:** MRI image of skull metastasis detected in *BRAF/p53* mouse on dox for 13 weeks. *Right:* Regression after 6 weeks off dox.



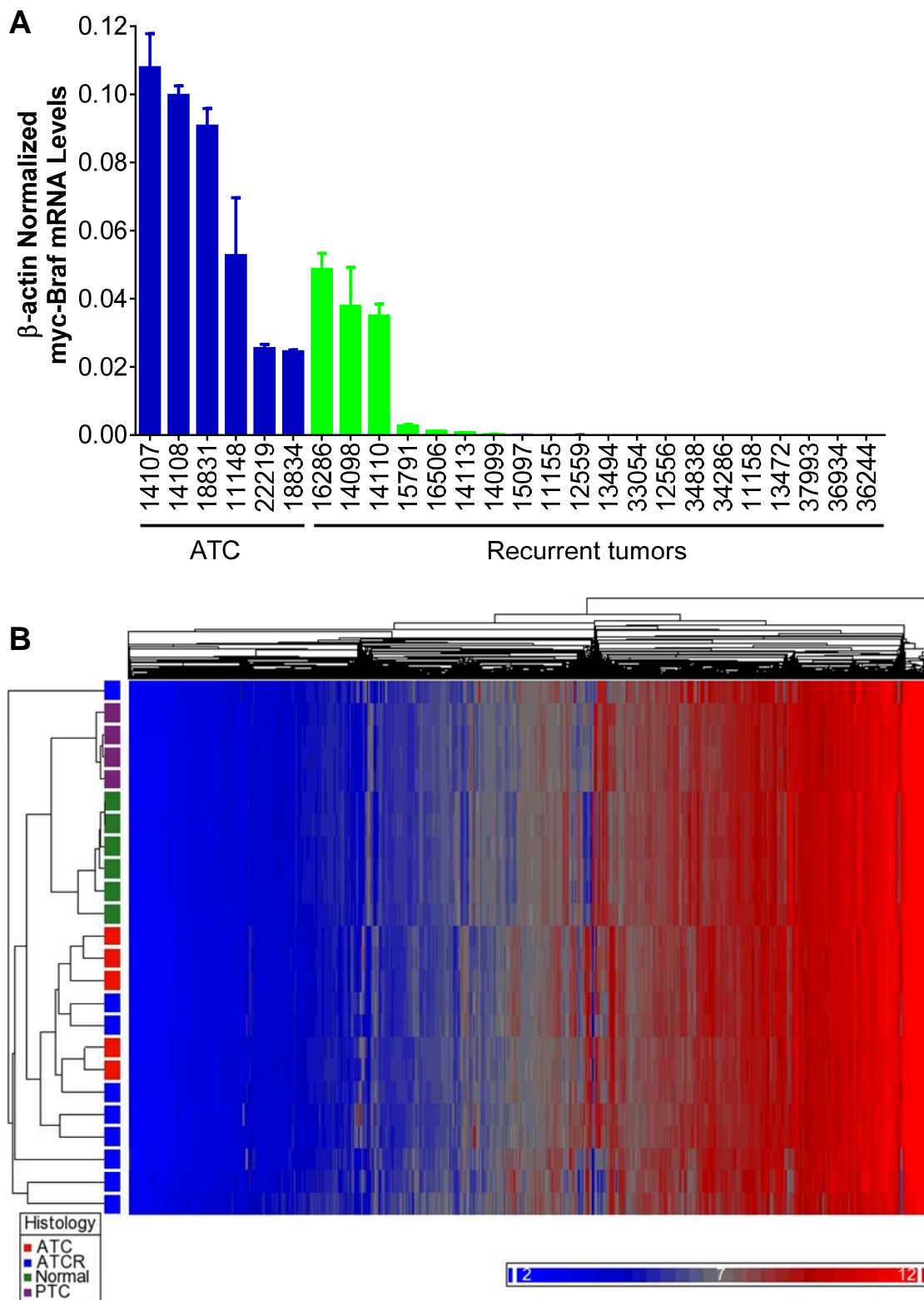
Supplemental Figure 4: *Tumor remnants after dox withdrawal consist primarily of fibrotic tissue with small foci of tumors cells.* **A)** Representative images of H&E staining of ATC remnants 3-6 weeks after dox withdrawal showing marked fibrosis with small foci of thyroid cells with features consistent with PTC (a, arrow: nuclear groove), PDTC (b, arrow: necrosis) or ATC (c, arrow: spindle-shaped cancer cell). **B)** H&E and IHC for pERK and Myc-tag (for myc-tagged BRAF^{V600E}) in a representative ATC on dox and a tumor remnant 6 weeks after dox withdrawal.



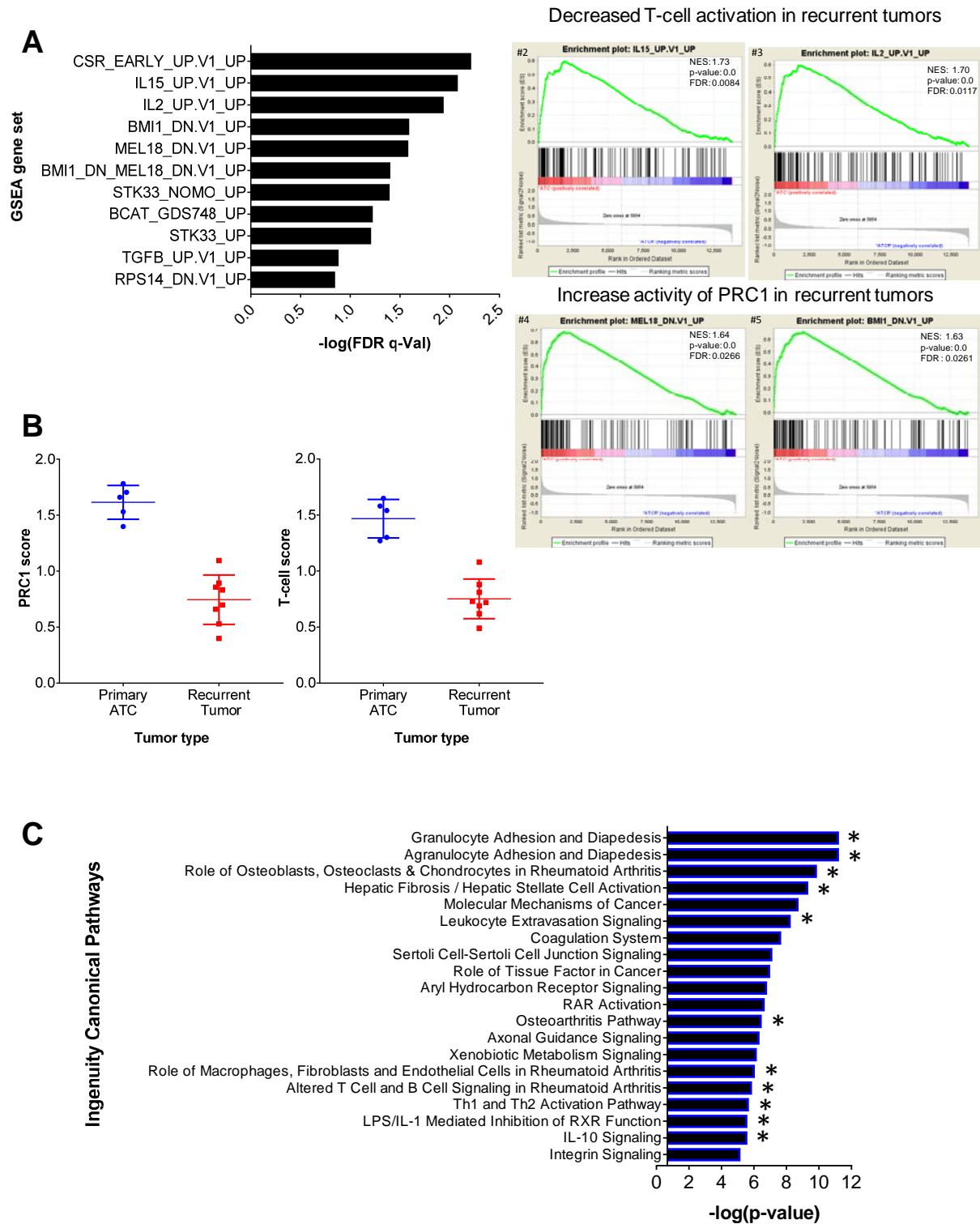
Supplemental Figure 5: *Diverse histological features of ATCs recurring after dox withdrawal:* H&E stained sections from representative recurrences with various histopathologies. a) Adenocarcinoma with mucin production (2 of 22; arrow: tumor cell with intracytoplasmic mucin); b) PDTc (5 of 22; arrow: necrosis); c) ATC with osteosarcoma transdifferentiation (2 of 22; arrow: osteoid laid by ATC cells); d) Spindle cell ATC with PTC component (arrow: PTC; star: ATC); e) Spindle cell ATC with mitosis (arrow: mitotic tumor cell).



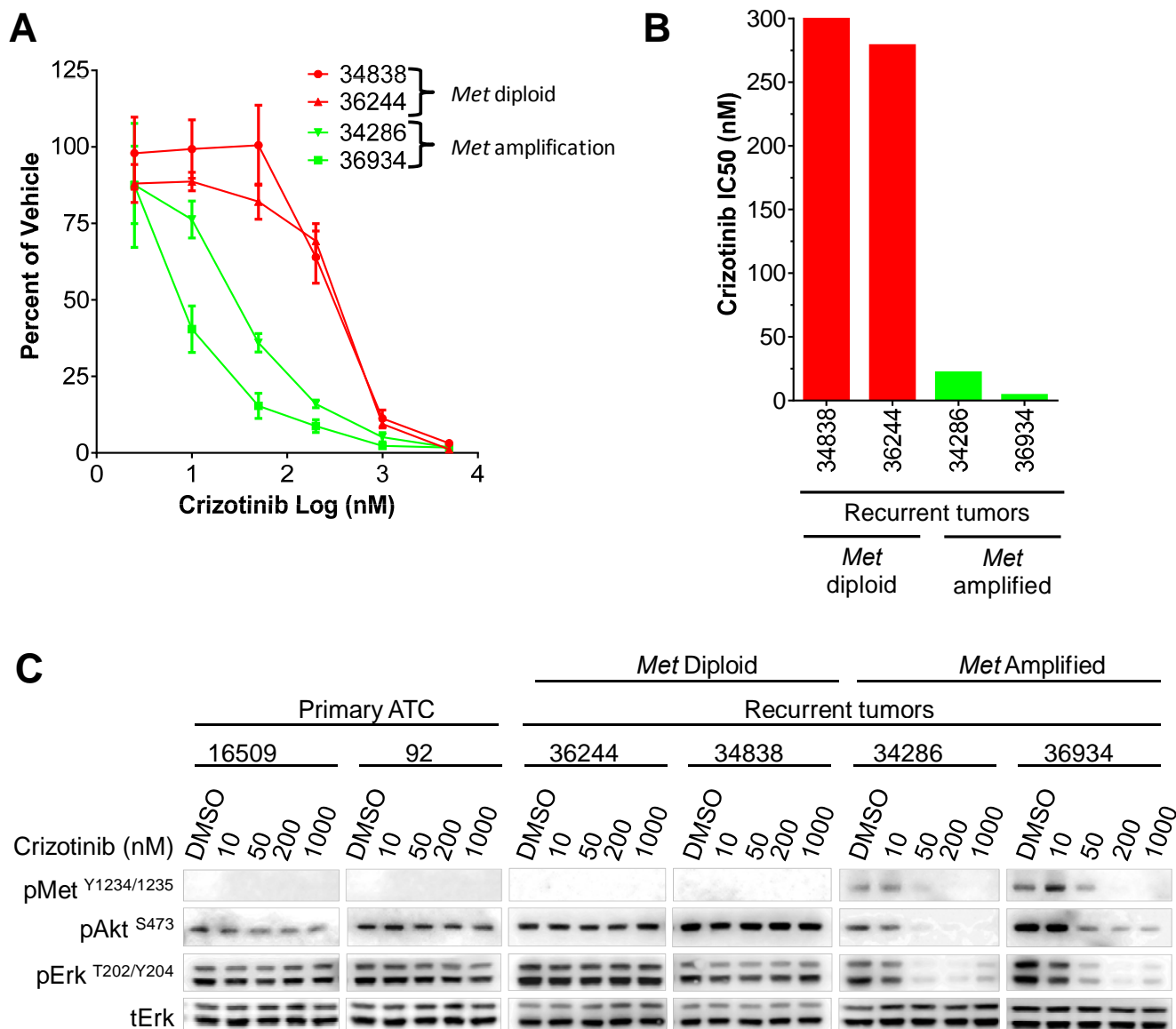
Supplemental Figure 6: *Prolonged tumor dormancy after dox withdrawal:* MRI images of *BRAF/p53* mouse over time: **A)** ATC after 8 weeks on dox. **B)** Tumor regression after 3 weeks off dox. **C)** No recurrence after 75 weeks off dox. **D)** Recurrent disease 2 weeks after switching back to dox diet. **E)** Second round of dox withdrawal for 3 weeks did not promote tumor regression.



Supplemental Figure 7: Gene expression profiling uncovers heterogeneity in mouse ATC recurrent tumors: A) RT-PCR with primers specific to myc-tagged BRAF^{V600E} cDNA in primary ATCs and recurrent tumors. All but 3 of the recurrent tumors lacked expression of the transgene. Three of the recurrent tumors expressed BRAF^{V600E} in a dox-independent manner. **B)** Unsupervised hierarchical clustering of gene expression separates normal thyroid, BRAF-PTCs and BRAF-ATCs. ATC recurrences cluster away from the other groups and from each other consistent with divergent mechanisms driving resistance to loss of BRAF^{V600E}.



Supplemental Figure 8: Increased PRC1 complex activity and reduced T cell activation in recurrent tumors. **A)** GSEA of gene expression profiles of recurrent (n=8) vs primary ATCs (n=5). Left) Top 10 gene sets. Right) GSEA enrichment plots for 4 of the 5 top-ranked gene-set signatures. IL15 and IL2 mark T cell activation; MEL18 and BMI1 are components of the polycomb repressor 1 complex (PRC1). **B).** T-cell and PRC1 transcriptional scores in primary and recurrent ATCs. **C)** Top 20 ranked Ingenuity canonical pathways differentially regulated between recurrent tumors and primary ATCs. *pathways consistent with reduced immune response in recurrent tumors.



Supplemental Figure 9: Met amplified recurrences are sensitive to crizotinib. **A)** Growth of *Met* diploid and *Met* amplified relapsed ATC cell lines 6 days after incubation with the indicated dose of crizotinib. **B)** Crizotinib IC₅₀ for the indicated cell lines. **C)** Dose response of 1 hour treatment with crizotinib on *Met* phosphorylation and downstream signaling in recurrent ATC cell lines with or without *Met* amplification.